The Benzophenone $S_1(n,\pi^*) \rightarrow T_1(n,\pi^*)$ States Intersystem Crossing Reinvestigated by Ultrafast Absorption Spectroscopy and Multivariate Curve Resolution

Stéphane Aloïse,* Cyril Ruckebusch, Lionel Blanchet, Julien Réhault, Guy Buntinx, and Jean-Pierre Huvenne

Laboratoire de Spectrochimie Infrarouge et Raman (CNRS UMR 8516), Centre d'études et de recherches Lasers et Applications (CNRS FR 2416), Université des Sciences et Technologies de Lille, Bat C5, 59655 Villeneuve d'Ascq Cedex, France

Received: July 24, 2007; In Final Form: October 19, 2007

The well-known benzophenone intersystem crossing from $S_1(n,\pi^*)$ to $T_1(n,\pi^*)$ states, for which direct transition is forbidden by El-Sayed rules, is reinvestigated by subpicosecond time-resolved absorption spectroscopy and effective data analysis for various excitation wavelengths and solvents. Multivariate curve resolution alternating least-squares analysis is used to perform bilinear decomposition of the time-resolved spectra into pure spectra of overlapping transient species and their associated time-dependent concentrations. The results suggest the implication of an intermediate (IS) in the relaxation process of the S_1 state. Therefore, a two step kinetic model, $S_1 \rightarrow IS \rightarrow T_1$, is successfully implemented as an additional constraint in the soft-modeling algorithm. Although this intermediate, which has a spectrum similar to the one of $T_1(n,\pi^*)$ state, could be artificially induced by vibrational relaxation, it is tentatively assigned to a hot $T_1(n,\pi^*)$ triplet state. Two characteristic times are reported for the transition $S_1 \rightarrow IS$ and $IS \rightarrow T_1$, ~6.5 ps and ~10 ps respectively, without any influence of the solvent. Moreover, an excitation wavelength effect is discovered suggesting the participation of unrelaxed singlet states in the overall process. To go further discussing the spectroscopic relevancy of IS and to rationalize the expected involvement of the $T_2(\pi,\pi^*)$ state, we also investigate 4-methoxybenzophenone. For this neighboring molecule, triplet energy level is tunable through solvent polarity and a clear correlation is established between the intermediate resolved by multivariate data analysis and the presence of a $T_2(\pi,\pi^*)$ above the $T_1(n,\pi^*)$ triplet. It is therefore proposed that the benzophenone intermediate species is a $T_1(n,\pi^*)$ high vibrational level in interaction with $T_2(\pi,\pi^*)$ state.

1. Introduction

The relaxation of the photoexcited $S_1(n,\pi^*)$ state of benzophenone (BP) and other related molecules is one of the most important photophysical processes within the field of organic photochemistry due to its fundamental role in photoreactivity of aromatic ketones. Many time-resolved absorption studies[1−7] have dealt with this subject, and the main results can be summarized as follows: (i) the $S_1(n,\pi^*)$ state decay gives rise to the triplet $T_1(n,\pi^*)$ state through intersystem crossing (ISC) process; (ii) a unique ~10 ps characteristic time describes this dynamic with a quantum yield close to unity and does not depend on the excitation wavelength; (iii) the commonly admitted non-solvent dependency[1−5] of the process has been questioned recently;[6] (iv) the observation of a blue shift[2,5] during the growth of triplet state absorption spectra has been contradicted[3] raising the question of vibrational relaxation engagement in the $S_1 \rightarrow T_1$ transition.

The photophysical issue discussed in this article is related to the fact that the very fast ISC process observed for the BP $S_1(n,\pi^*)$ state is in contradiction with the El-Sayed rules, predicting a slow process for the forbidden n,π^*-n,π^* transition. In fact, controversy still exists regarding the exact photophysical mechanism of the S_1 state relaxation process. On one hand, some explanations rely on the participation of the $T_2(\pi,\pi^*)$ state ensuring $S_1(n,\pi^*) \rightarrow T_2(\pi,\pi^*)$ ISC then followed by an ultrafast $T_2(\pi,\pi^*)-T_1(n,\pi^*)$ internal conversion (IC).[8] Very recently, this photophysical scheme was confirmed by Yabumoto et al. through their observation of the T_1-T_2 absorption band detected by time-resolved infrared absorption experiments.[9] On the other hand, low field Zeeman experiments performed at very low temperatures have totally ruled out the participation of a triplet intermediate during ISC of BP strongly suggesting a direct $S_1(n,\pi^*) \rightarrow T_1(n,\pi^*)$ mechanism.[10] Furthermore, optically detected magnetic resonance (ODMR) and related experiments have given evidence of $(n,\pi^*-\pi,\pi^*)$ configuration mixing for the lowest triplet state, which allows direct ISC to occur.[11] To further discuss the controversy, new subpicosecond time-resolved absorption experiments combined with advanced multivariate curve resolution for data analysis are attempted to investigate the BP photophysics relaxation of the $S_1(n,\pi^*)$ state.

In numerous chemical fields, multivariate curve resolution—alternating least squares (MCR-ALS)[12,13] is becoming the standard chemometric method to resolve multicomponent evolving systems into pure contributions. Some convincing results have been obtained in the field of time-resolved spectroscopy,[14,15] but to our knowledge spectral and temporal characterizations of ultrafast transient species was only attempted very recently.[16] Multivariate curve resolution aims to perform decomposition of kinetic data matrix D (i.e., a set of individual spectra probed at different time delays, $\{\Delta OD(t,\lambda)\}$) into pure spectra of overlapping transient species and their associated time-dependent concentrations, without specifying any phe-

* Corresponding author. E-mail: stephane.aloise@univ-lille1.fr.

10.1021/jp075829f CCC: $40.75
Published on Web 12/22/2007

nomenological model. More precisely, only the assumption of a bilinear decomposition of the data set into additive contributions of concentration and spectra is underlying. The originality with regard to global analysis[17] and target data analysis[18] relying on the same mathematical decomposition is that the proposed method is basically soft-modeling. Indeed, only initial estimation of the concentration profiles or spectra are to be input in MCR-ALS, which thus do require the number of significant contributions to the signal (the rank of *D*) to be estimated using singular value decomposition (SVD).[20] But bilinear decomposition of *D* must be constrained in order to limit rotational ambiguities.[12] Basically, soft-modeling constraints[12,21] are nonparametric information, e.g., non-negativity of the concentration profiles and spectra, that are implemented during the ALS optimization to focus on chemically meaningful data decomposition. Multivariate curve resolution enables one to decompose the phenomena describing the measured data, but the interpretation of the results should be done with caution, as in the other more conventional data analysis.[19] When a kinetic model is suspected, a step forward is the consideration of kinetic constraints[22] implemented on the concentration profiles in the ALS algorithm. An advantage from the photophysical point of view is that the rate constants[22,23] of the model implemented can be obtained as additional information. From the point of view of chemometrics, this so-called hard−soft multivariate curve resolution (HS-MCR) provides solutions with very small ambiguity. In particular, when combined with the application of soft-modeling non-negative constraints to the pure spectra, the slow−fast ambiguity associated with several model fits of successive first-order reactions can be accounted for.

The present paper aims at gaining a better understanding of the $S_1 \rightarrow T_1$ photophysical process for the BP molecule through multivariate curve resolution of subpicosecond time-resolved absorption data for various solvents and excitation wavelengths. The results obtained are compared with similar spectroscopic data acquired for 4-methoxybenzophenone (4-MeOBP). Indeed, for the latter compound, Boscà et al. have demonstrated recently a T_1-T_2 triplet state inversion induced by the solvent polarity,[24] allowing different El-Sayed schemes to be tested including the one for BP.

2. Experimental Methods

2.1. Experimental. The pump−probe subsubpicosecond absorption experiments were carried out using an amplified Ti: sapphire laser (BM Industries) delivering 0.8 mJ and 80 fs pulses tunable between 766 nm and 800 nm with a repetition rate of 1 kHz. The 383 nm pump pulses were obtained by frequency doubling the fundamental at 766 nm while the 267 nm pump pulses were obtained by frequency tripling the fundamental at 800 nm. Energies higher than 20 μJ were provided in both cases. The probe beam was generated by focusing 1 μJ of the fundamental on a 1 mm CaF_2 plate giving a white light continuum with a spectrum covering the UV−vis and near IR range. The probe beam was split into signal and reference beams before crossing the sample, and the resulting beams were recorded on 2 different channels of a multichannel spectrograph equipped with a CCD camera. Transient absorbance was obtained by comparing signal and reference spectra for different time delays. The time delay between the pump and probe was varied up to 1.5 ns (using a micrometric optical delay line), and the temporal resolution of the apparatus was better than 300 fs. Pump and probe beams, with relative linear polarizations set at the magic angle, were focused in a 2 mm flow cell equipped with CaF_2 windows. Typical sample concentrations used were 5×10^{-4} M for 267 nm excitation and 0.2 M for 383 nm excitations. The following Sigma-Aldrich products were used: benzophenone, 4-methoxybenzophenone, acetonitrile (ACN), methanol (MeOH), dichloromethane (CH_2Cl_2) and cyclohexane (CH). All solvents (spectroscopic grade) were used without further purification.

2.2. Data Analysis. The basic mathematical model is a bilinear decomposition of the data matrix **D** according to eq 1, in matrix notation. The matrix **D** (with elements d_{ij}) contains *i*

$$\mathbf{D} = \mathbf{C}\mathbf{S}^{\mathbf{T}} + \mathbf{E} \tag{1}$$

spectra recorded at *i* successive delay times and *j* wavelengths. The matrix **C** (elements c_{jk}) contains the resolved concentration profiles (*i* time points) of the *k* components contributing to **D**. The matrix $\mathbf{S}^{\mathbf{T}}$ (elements s_{kj}) contains the corresponding *k* pure spectra. The matrix **E** (elements e_{ij}) contains the residuals of the decomposition. MCR-ALS can be used to solve the bilinear model eq 1, i.e., to extract **C** and $\mathbf{S}^{\mathbf{T}}$ from **D**. The striking aspects of the methodology (applied to time-resolved spectroscopic data) are given below.

Singular Value Decomposition and Related Methods. In any data analysis strategy,[12,18] the first point is to estimate the number of components (transient species) composing the observable **D**. This is usually performed analyzing the chemical rank of **D** using SVD[25] and determining the number of significant singular values. In practice, different kinds of difficulties may appear. The most common one is to settle correctly the threshold that separates chemical contribution from noise in the SVD. Moreover, strong overlapping of the concentration profiles and high intrinsic collinearity of the spectra may blur the situation. However, when two-way data matrices are studied as in time-resolved spectroscopy, advantage can be taken from evolving factor analysis methods such as the so-called evolving factor analysis (EFA).[26] This procedure, instead of calculating SVD or principal component analysis[20] (PCA) of the full data matrix, performs successive analysis on gradually increasing submatrices in the time direction, adding a row at a time from the top of the matrix to the bottom (forward EFA). The emergence and evolution of the singular values can thus be followed individually with increasing time. The same approach is performed from bottom to top (backward EFA). In this case, the emergence and evolution of the singular values can be followed in reverse sequence, i.e., their disappearance can be observed with increasing time. Under the assumption that the evolving system studied is sequential, i.e., the first compound to appear is also the first to disappear, estimation of the profiles **C** can be provided combining the forward and backward traces. It can then be input as initial solution in the MCR-ALS procedure.

Multivariate Curve Resolution−Alternating Least Squares. An alternating least squares (ALS) algorithm is used to fit iteratively the **C** and $\mathbf{S}^{\mathbf{T}}$ matrices to the experimental data **D**. The residuals are obtained computing the difference between the data **D** and the reproduced data $\mathbf{CS}^{\mathbf{T}}$. At each iterative cycle of the optimization, matrices **C** and $\mathbf{S}^{\mathbf{T}}$ are calculated under constraints minimizing the reproduction error, **E**. The lack of fit (eq 2) can be used as global estimator of the fitting error of the experimental data.

$$\text{lof}\,(\%) = 100\sqrt{\frac{\sum_{i,j} e_{i,j}}{\sum_{i,j} d_{i,j}}} \qquad (2)$$

The full MCR-ALS procedure can be cast as follows: (1) determination of the number of components contributing to **D**; (2) construction of initial estimates of concentration profiles **C** using chemical insight or chemometric methods such as EFA; (3) given **D** and **C**, least-squares calculation of $\mathbf{S^T}$ under suitable constraints; (4) given **D** and $\mathbf{S^T}$, least-squares calculation of **C** under suitable constraints; (5) reproduction of **D** using **C** and $\mathbf{S^T}$. Check if the convergence criterion is fulfilled. If not, go back to step 3.

As there is no phenomenological (kinetic) model imposed in the decomposition, multivariate curve resolution is affected by rotational ambiguities, i.e., the possibilities to reproduce the original data sets with the same precision using **C** and $\mathbf{S^T}$ matrices that contain linear combinations of the signals of the pure components. The set of possible solutions can be restricted through the implementation of soft-modeling constraints[12,21] (steps 3 and 4), such as non-negativity, unimodality (single peak) or closure (mass balance). Additionally, such constraints ensure that the computed solutions are chemically meaningful.

Hard−Soft Multivariate Curve Resolution−Alternating Least Squares. Hard−soft Multivariate Curve Resolution (HS-MCR) is an evolution of soft-modeling MCR-ALS including hard-modeling constraint[22,23] that can be very useful in the analysis of time-resolved spectroscopy data sets. The optimization starts with the profiles obtained from a soft-modeling MCR-ALS resolution. These profiles are used as input of the HS-MCR algorithm. Then, a kinetic model can be incorporated by means of a hard-modeling kinetic constraint which is applied on the matrix of concentration profiles (step 4 of the MCR-ALS algorithm presented above). Inside each loop of the ALS procedure, the columns of **C** are fitted to the model and the resulting profiles are used to calculate the spectra $\mathbf{S^T}$, deriving advantage from soft-modeling resolution as well. The reliability of the soft modeling solutions[27] can then be discussed, and time constants can be estimated. The confidence intervals calculated with the standard deviations of the fitted parameters are given for information only as they can be seriously underestimated (due to cross-correlations between the parameters).[28] More generally, with regard to classical hard-modeling, HS-MCR has been shown to be much more flexible[22,23] as the columns of **C** can be constrained one independently of the others making it possible to handle interferents for example.

All the calculations have been performed using MATLAB 6.5 and 7.0 (R14) (The Matworks Ltd, Massachusetts). The interface of MCR-ALS is freely available at www.ub.es/gesq/mcr/mcr.htm.

3. Results and Discussion

In the following, subpicosecond time-resolved absorption data of BP obtained for various solvents and excitation wavelengths will be presented. The time-resolved spectra are first analyzed in a conventional way, fitting kinetic traces by monoexponential function at chosen wavelengths (section 3.1). The multivariate curve resolution analyses of the experimental data sets are then performed. The results obtained from both MCR-ALS and HS-MCR are discussed (section 3.2). In order to obtain a chemical validation of the results obtained for BP, a similar approach is applied to 4-MeOBP. Indeed, the neighboring photophysics of this compound is solvent-dependent and can thus be controlled. Finally, the S_1 state photophysics of BP is discussed in light of the new results obtained (section 3.3).

3.1. Conventional Interpretation of Time-Resolved Spectra. The raw (no smoothing applied) transient absorption spectra of BP compound in acetonitrile (0.2 M) at 383 nm excitation recorded in the 420−680 nm spectral range and in the 0.8−100 ps time window are shown in Figure 1. The first short delay times spectrum characterizes the $S_1(n,\pi^*)$ visible spectrum of BP peaking at $\lambda_{max} = 570$ nm (see 0.8 ps trace), as reported elsewhere.[4] It then decreases while the well-known $T_1(n,\pi^*)$ absorption spectrum peaking at $\lambda_{max} = 525$ nm increases. On one hand, the $S_1(n,\pi^*)$ characteristic time can be estimated (monoexponential fitting) at 570 nm to (17 ± 1) ps (see inset). On the other hand, fitting the kinetic growth at 525 nm returns the value (9.4 ± 0.3) ps, in agreement with other studies,[7] but it gives no evidence of a direct S_1-T_1 transition. When the experiment is repeated changing the solvent, the $T_1(n,\pi^*)$ state characteristic growing time is estimated at 525 nm to be (11.6 ± 0.3) ps for MeOH and (11.8 ± 0.3) ps for CH_2Cl_2. This confirms that the apparent ISC process is neither very sensitive to hydrogen bonding ability nor to solvent polarity, as previously reported.[1−5]

The transient absorption spectra of BP obtained for 267 nm excitation in the case of acetonitrile (5×10^{-4} M) are displayed in Figure 2 for a wider spectral range (320−680 nm). The 0.8−1.7 ps time delay (see inset) shows the fast growth of the $S_1(n,\pi^*)$ spectra at 570 nm following the $S_2(n,\pi^*) \rightarrow S_1(n,\pi^*)$ IC process in accordance with the S_2 lifetime of 0.53 ps[7] measured by Shah et al. (in the following, only time delays greater than 2 ps will be considered in order to get rid of the S_2 state contribution). Besides the appearance of the triplet spectra with a characteristic time of (10.9 ± 0.3) ps, the blue band of $S_1(n,\pi^*)$ spectra peaking at 330 nm is observed to be decreasing with a decay time of (10.2 ± 0.5) ps. So, if one considers only these two bands at 330 and 525 nm wavelengths, and ignores the observations just made above, a direct $S_1 \rightarrow T_1$ transition can be assumed for the 267 nm excitation case.

Another important issue concerns the blue shift during the growth of the triplet absorption band around 525 nm. Unlike Hamanoue et al.,[3] a slight shift is observed for 383 nm excitation which is clearly more pronounced for 267 nm excitation. This spectral effect has been previously interpreted in terms of vibrational relaxation of the triplet state.[2] More recently, it has been proposed that the decay of the singlet (band at 570 nm) and the growth of the triplet appear as a blue shift in the observed spectra.[4] One of the advantages using MCR-ALS is to improve the rationalization of such a weak spectral effect.

3.2. Multivariate Curve Resolution of Time-Resolved Spectra. Multivariate curve resolution of the data matrix corresponding to BP transient absorption spectra at 267 nm excitation is presented first. SVD and EFA are performed to estimate the number of significant contributions to consider for the description of the S_1 state relaxation mechanism. The EFA results are displayed in Figure 3. The plot represents the PCA eigenvalues (in log units) as a function of the position of the considered row in the data matrix (row number), which corresponds to time direction. As an example four eigenvalues are calculated at 4 ps since a 4-row submatrix is considered (see forward EFA full-lines). Moreover, if row number 21 is considered (conversely, row number 2 in backward analysis, see dotted lines) the calculated values correspond to PCA or SVD (it is reminded here that eigenvalues are scarred singular

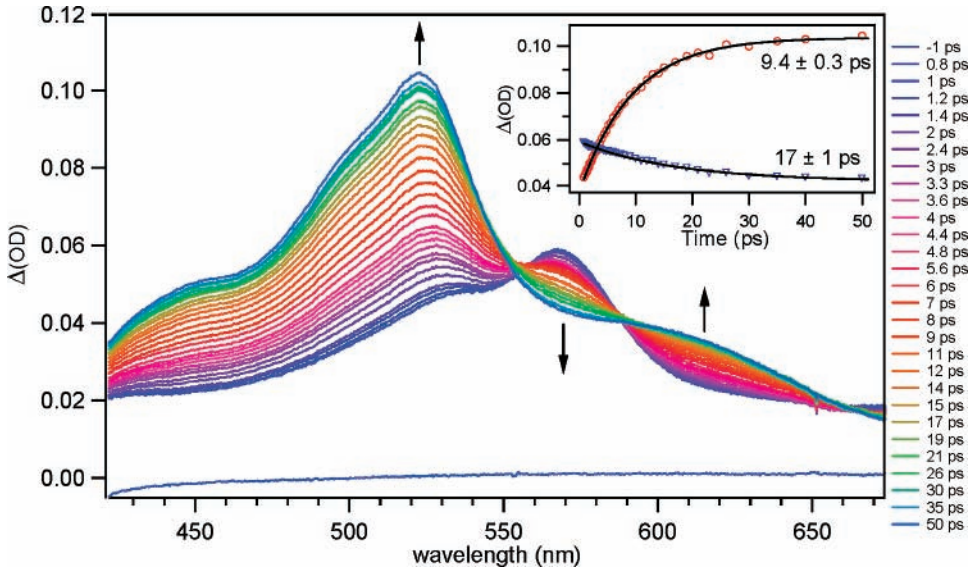

Figure 1. Subpicosecond time-resolved absorption spectra of BP in ACN for 383 nm excitation in the 0.8−50 ps temporal window. The time evolution is shown by arrows. The inset displays the kinetic traces and monoexponential fit at 525 nm (red circles) and 570 nm (blue inverted triangles).

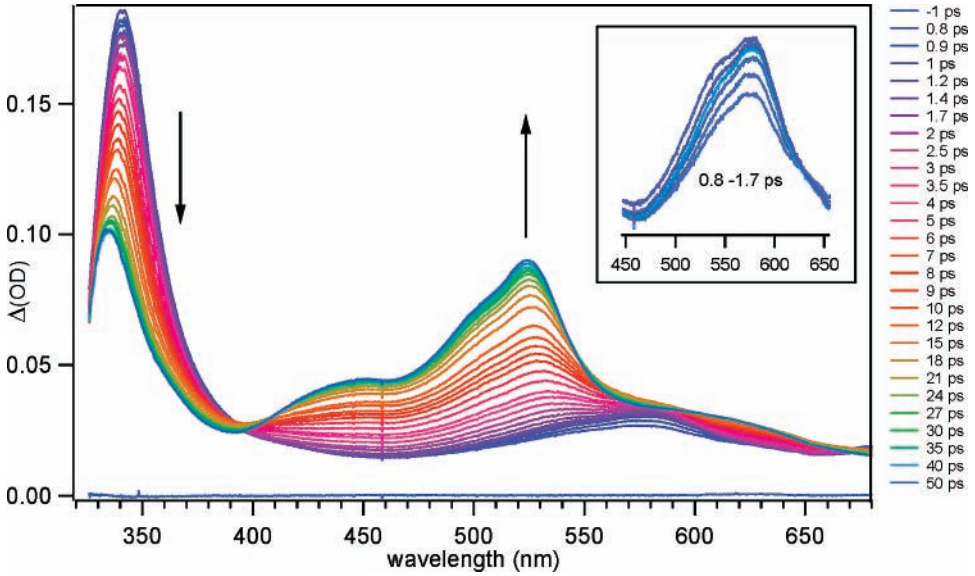

Figure 2. Subpicosecond time-resolved absorption spectra of BP in ACN for 267 nm excitation in the 0.8−50 ps temporal window. The time evolution is shown by arrows. The inset is a zoom of the 450−650 nm regions for the indicated time window.

values) of the full data matrix. A threshold separating minor contributions can be set at ∼−3.4 (in log units), and three contributions are thus found significant. Besides, EFA provides more information as it takes into account the intrinsic temporal evolution of the data matrix. In forward direction, it can then be observed that the second contribution emerges very quickly (<2.5 ps) whereas as the third is significant after ∼10 ps. This third forward trace is a reasonable initial estimate of the kinetic profile of the third contribution involved in the process analyzed. In backward direction, the same analysis returns, for example, the third profile is significantly present only before ∼12 ps and it provides an initial estimate of the profile corresponding to the first contribution (i.e., its disappearance). Finally, combining the second forward and backward traces, an initial estimate of the evolution of an intermediate contribution is observed.

The results of soft-modeling MCR-ALS analysis based on initial estimate from EFA are now discussed. The constraints implemented during the ALS optimization are non-negativity of the concentration profiles and spectra and unimodality of the concentration profiles. The results obtained for BP spectra at 267 nm excitation are given in Figure 4a and 4b for the pure spectra ($\mathbf{S}^T$) and the corresponding time-dependent concentration ($\mathbf{C}$), respectively. First, the initial $S_1(n,\pi^*)$ spectra (in blue; λ_{max}∼330 and ∼570 nm) and the final $T_1(n,\pi^*)$ spectra (in red; λ_{max}∼325 and ∼525 nm) are unambiguously recognized. Meanwhile, the corresponding concentration profiles are found relevant since the disappearance of $S_1(n,\pi^*)$ (blue circles) is concomitant with the appearance of $T_1(n,\pi^*)$ (red squares). Apart from these two species, an intermediate contribution is resolved, which is denoted by IS in the following. The corresponding spectrum (in green in Figure 4a) peaks in the visible region at higher wavelength compared to $T_1(n,\pi^*)$, i.e., $\Delta\lambda_{max}(IS-T_1) = 13$ nm. Similar comparison with the $S_1(n,\pi^*)$ spectrum gives $\Delta\lambda_{max}(S_1-IS) = 41$ nm. Both the values are reported in Table 1. The corresponding time-dependent concentration profile (green triangles in Figure 4b) is found to be in agreement with the EFA results. This resolution introduces the implication of a direct intermediate species in the $S_1(n,\pi^*)$

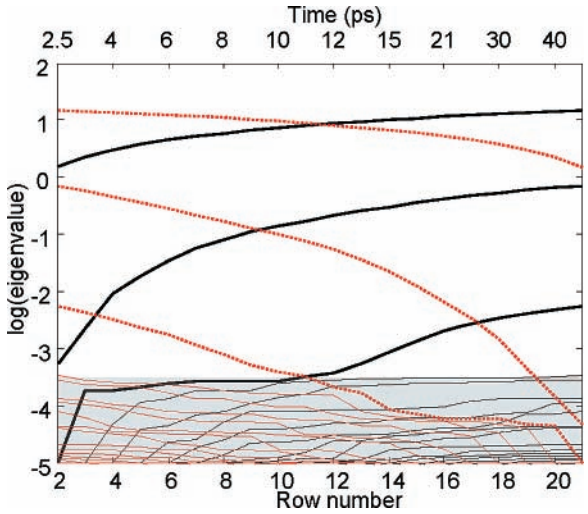

Figure 3. Evolving factor analysis (EFA) for subpicosecond time-resolved absorption data of BP (267 nm excitation; see Figure 2); results of forward (solid lines) and backward (dashed lines) EFA; eigenvalues (in log units) are plotted as a function of the row number of the data matrix and corresponding time (the shadowed region is set to figure out significant contributions).

$\rightarrow T_1(n,\pi^*)$ transition. To support this result, the HS-MCR procedure is then performed. In addition to the non-negativity constraints applied to the pure spectra as mentioned previously, a kinetic constraint which describes the sequential two step kinetic model proposed in eq 3 is considered. The results are

$$S_1(n,\pi^*) \rightarrow IS \rightarrow T_1(n,\pi^*) \quad (3)$$

plotted in Figure 4a,b (black lines) for spectral and time-dependent concentration profiles, respectively. Excellent agreement is found with previous MCR-ALS results. The reliability of the two step kinetic scheme implemented is demonstrated for BP time-resolved absorption spectra (267 nm excitation), at least from a mathematical point of view. The rate constants for the $S_1 \rightarrow IS$ process, denoted by k_1, is (0.154 ± 0.002) ps^{-1} and for the $IS \rightarrow T_1$ process, denoted by k_2, is (0.093 ± 0.001) ps^{-1}. These values (reported in Table 1) will be discussed in section 3.3. It should be noticed that the application of soft-modeling non-negativity constraint to the spectra enables one to avoid the slow−fast ambiguity (also known as flip-flop phenomenon, such an effect is observed when the rate constants describing a multistep reaction scheme can be interchanged giving an equivalent solution for the fitting). Indeed, this can be verified by checking that the solution obtained is maintained when the model is refit with the constraint turned off.[29]

The same procedure is repeated for BP at 383 nm excitation, and the results are displayed in Figure 4c,d for $\mathbf{S^T}$ and $\mathbf{C}$, respectively. First, comparing the $\Delta\lambda_{max}$ calculated with the previous ones (see Table 1), a comparable value for S_1-IS (40 nm) is obtained while a factor of about 2 is noticed for $IS-T_1$ (5 vs 13 nm). On the other hand, the concentration profiles obtained from soft-modeling MCR-ALS and from HS-MCR under the constraint eq 3 are found consistent despite slight differences (the resolution is more challenging as the wavelength domain is narrowed). Finally, the values obtained for k_1, (0.133 ± 0.002) ps^{-1}, and k_2, (0.099 ± 0.001) ps^{-1} (Table 1), are in good agreement with the previous case.

3.3. The Benzophenone $S_1 \rightarrow T_1$ ISC Process. At this point, whether the intermediate species (IS) is a true spectroscopic state or not has to be discussed. What is its chemical relevance, and to what extent might vibrational relaxation of S_1 or T_1 states contribute[2−6] to the MCR-ALS spectra of IS? Before beginning such a discussion, it is important to remember that IS is recovered under the assumption of a bilinear decomposition of the data (see eq 1). It means that significant collective processes such as pure vibrational effect or excited-state solvation (inducing spectral band shift, see for example ref 30) can hardly be included in a 3 component resolution. In any case, among these two types of processes, the solvation effects have never been reported for BP.

The first striking aspect of IS is that its full spectrum is very similar but broader compared to the T_1 state spectrum. In light of this argument, there are two possible explanations concerning the chemical relevancy of IS: (i) IS is a mathematical artifact induced by pure vibrational relaxation during a direct ISC from S_1 to T_1 states (one electronic transition); (ii) the IS species is related to one or several vibrational states in the $T_1(n,\pi^*)$ manifold, i.e., IS is a hot triplet state that is involved in a two step mechanism (two electronic transition). We do not believe that we can give a final answer to this dilemma, but we want to insist on the good agreement between the soft-modeling results (without any model prerequisites) and the ones constrained to follow a two step sequential model. In our opinion, such an agreement would not be obtained in case the blue shift observed during growth of T_1 was due to pure vibrational effect alone.[2,5]

Furthermore, another meaningful result is the discovery of an excitation wavelength effect (see Table 1): $\Delta\lambda_{max}(IS-T_1)$ is more than two times larger comparing the 383 nm and 267 nm excitation cases (for ACN solvent). This difference stands for the fact that the S_1 state is populated near the $\upsilon = 0$ threshold for 383 nm excitation while numerous vibrational states can be populated by 267 nm excitation through the S_2-S_1 IC process. In terms of vibronic coupling, one explanation would be that some high vibrational levels in the S_1 manifold are in effective interaction with the triplet state vibrational levels. It is to be noted that the proposition of ISC that occurs for unrelaxed singlets has been already proposed by Sun et al. in the past.[31]

Let us assume now that the characterized intermediate species is chemically relevant. Can it be related to the $T_2(\pi,\pi^*)$ state, as already proposed in the litterature?[8,9] Among unsuccessful experimental attempts to locate directly the $T_2(\pi,\pi^*)$ state,[32] the dual phosphorescence of BP in polar solvent is one of the most striking pieces of evidence of the simultaneous population of both (n,π^*) and (π,π^*) triplet states[33] allowing one to presume about some participation of the $T_2(\pi,\pi^*)$ state in the photophysics of singlet states. As we will see, the study of 4-MeOBP in CH, ACN and ACN/water (1:3) solvent by ultrafast absorption spectroscopy coupled with multivariate curve resolution analysis will help to bring some insights about this issue. Indeed, as Boscà et al.[24] demonstrated recently (with laser flash photolysis and phosphorescence measurements), the 4-MeOBP possesses the property to get the $T_2(\pi,\pi^*)-T_1(n,\pi^*)$ relative position varying with solvent polarity allowing different El-Sayed scheme to be probed. More precisely, for CH solvent, the (π,π^*) triplet state is well higher than the (n,π^*) triplet state, while for ACN, the gap between the two states is less than 8 $kJ\cdot mol^{-1}$ allowing vibronic coupling to occur. For solvents with the higher polarity, the triplet ordering is switched to the opposite situation and the lowest triplet state possesses then (π,π^*) character.[24] The subpicosecond absorption spectra obtained for 4-MeOBP in the three solvents and the corresponding MCR-ALS decompositions are presented all together in Figure 5. Note that HS-MCR analysis has not been performed because additional charge-transfer deactivation of the S_1 singlet excited state prevents the application of a simple kinetic mechanism.[34]

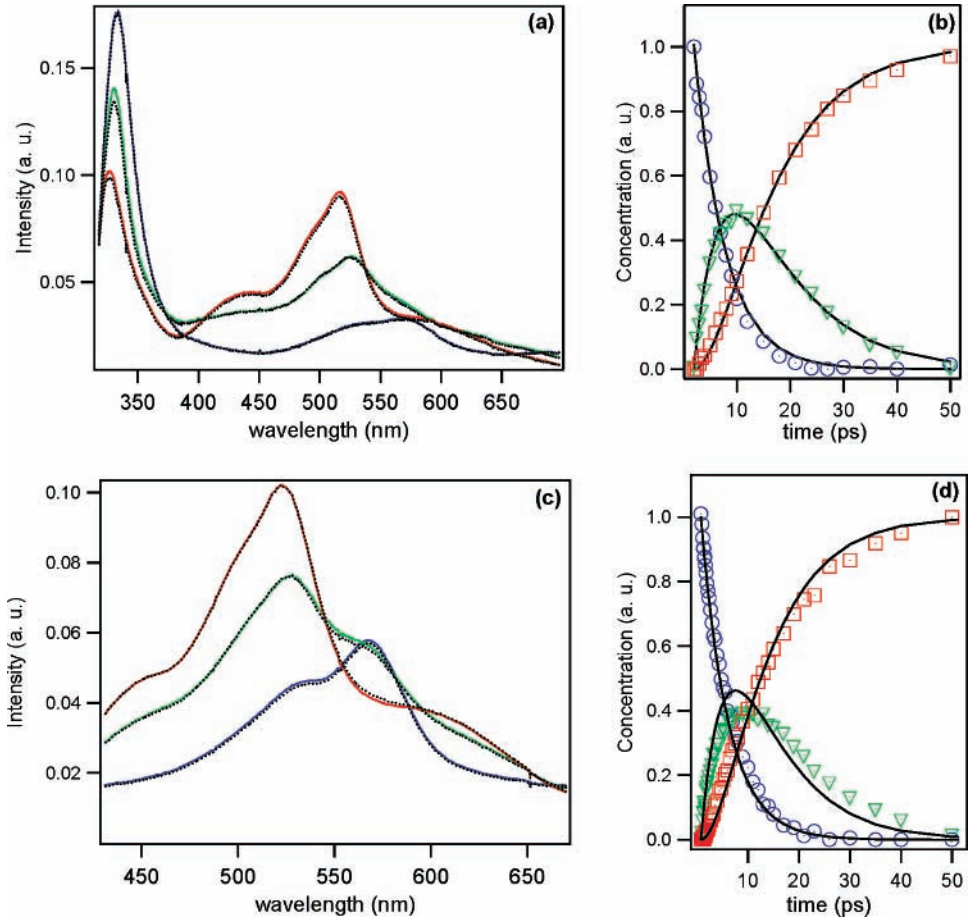

Figure 4. Spectra and time-dependent concentrations obtained from MCR-ALS (colored lines and markers, respectively) and from HS-MCR (black lines in both cases) analysis of subpicosecond time-resolved absorption data of BP excited at 267 nm, (a) and (b); and 383 nm, (c) and (d) in ACN. The color code is the following: blue for S_1; green for IS; red for T_1.

TABLE 1: Spectrokinetic Properties Obtained from HS-MCR Analysis of Subpicosecond Time-Resolved Spectra of BP for Different Solvents and Excitation Wavelengths

		$\Delta\lambda_{max}$ (nm)				
solvent	λ_{exc} (nm)	S_1-IS	$IS-T_1$	$S_1 \rightarrow IS$ k_1 (ps^{-1})[a]	$IS \rightarrow T_1$ k_2 (ps^{-1})[a]	lof (%)
ACN	267	41	13	0.154(2)	0.093(1)	0.59
ACN	383	40	5	0.133(2)	0.099(1)	0.92
MeOH	383	42	3	0.167(4)	0.117(3)	1.21
CH_2Cl_2	383	41	4	0.146(3)	0.103(3)	0.70

[a] Uncertainty estimations are given in parentheses (see ref 28 for more details).

For CH solvent, one observes the growth of the $T_1(n,\pi^*)$ triplet spectrum around 525 nm (Figure 5a) concomitant with the $S_1(n,\pi^*)$ spectrum disappearance at 340 nm. For ACN (Figure 5b), an additional shoulder peaking near 440 nm is clearly observed while for ACN:water (1:3) only the $T_1(\pi,\pi^*)$ triplet growth peaking at 440 nm is observed. All these results are in good agreement with the laser-flash photolysis spectra of Boscà et al. (see Figure 3 of ref 24). The inspection of the spectra and time-dependent concentration profiles obtained from multivariate curve resolution are proposed in Figure 5d−f. For the two cases where the (π,π^*) triplet is the highest state, three transient species are extracted (Figure 5d and 5e) with meaningful kinetics (see the insets). On the contrary, when the (π,π^*) triplet is the lower one, opening the possibility of a direct $S_1(n,\pi^*) \rightarrow T_1(\pi,\pi^*)$ ISC process allowed by El-Sayed rules, only two species are found significant in the EFA procedure and the corresponding MCR-ALS resolution is given in Figure 5f. This solution is very reliable, and attempts to force a 3-species resolution lead to meaningless results. So, on one hand, a clear correlation between the intermediate and the higher T_2 triplet state relative to T_1 can be established for 4-MeOBP. On the other hand, the similitude between the two IS spectra for BP (whatever the solvent) and 4-MeOBP in CH are particularly striking knowing that these two compounds have a quite similar energy ordering of the S_1, T_2 and T_1 states.[8,24] This last point makes an analogy between the two molecules reasonable, allowing one to assume that for BP the probable intermediate species during the ISC of $S_1(n,\pi^*)$ is also correlated with the presence of the $T_2(\pi,\pi^*)$ state above the final $T_1(n,\pi^*)$ triplet.

In fact, the two attempts performed in this section in order to assign IS are not exclusive: IS could be a hot $T_1(n,\pi^*)$ triplet state in strong vibronic interaction with the $T_2(\pi,\pi^*)$ state. The more pronounced (π,π^*) character for the high vibrational levels of T_1 states, by comparison with the ones near the vibrational threshold, would be conferred through the proximity of the two triplet states. This point is important in order to make the El-Sayed rules respected.

Within the indirect mechanism hypothesis for the S_1 state photophysics, i.e., IS is chemically relevant and attributed to be a mixture between hot $T_1(n,\pi^*)$ and $T_2(\pi,\pi^*)$ state, it becomes instructive to analyze the characteristic times (ignoring minor competitive processes, $\tau \approx 1/k$) given by the HS-MCR procedure. The S_1-IS and $IS-T_1$ transitions are characterized by mean times of ~6.5 ps and ~10 ps, respectively, irrespective of the solvent or excitation wavelength (see Table 1). The former time can be easily assigned to an ISC from $S_1(n,\pi^*)$ to IS which

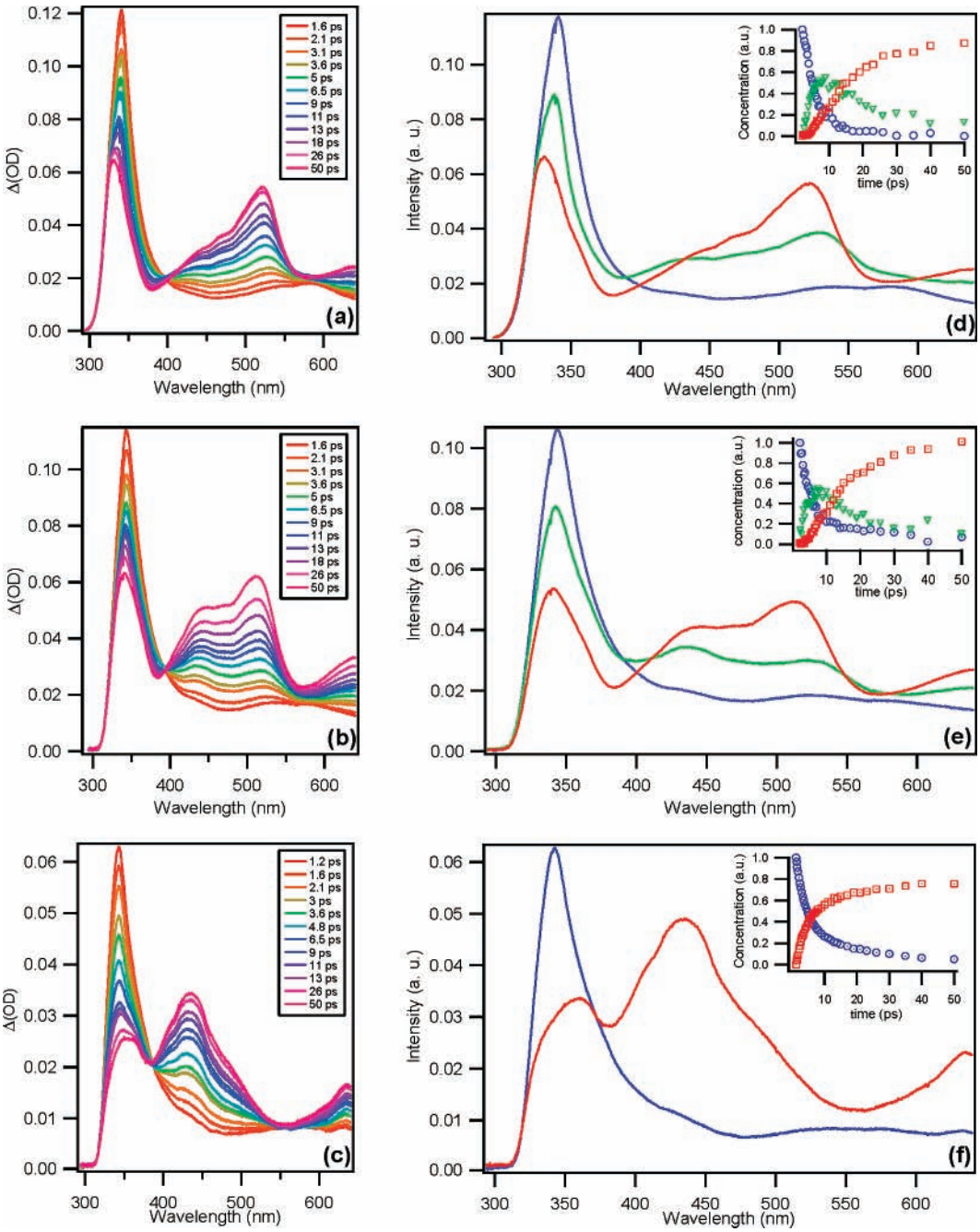

Figure 5. Subpicosecond time-resolved absorption data of 4-MeOBP excited at: 267 nm in CH (a), in ACN (b) and ACN/water 1:3 (c); respective spectra, (d), (e) and (f), obtained by MCR-ALS. The insets contain the time-dependent concentrations (same color code as for Figure 4).

is in the triplet manifold in all the considered situations. Considering the second transition like an IC from IS to the fully relaxed $T_1(n,\pi^*)$, much care has to be taken because of few published values in the literature for $T_2 \rightarrow T_1$ transition.[8] Due to the small gap between T_1 and T_2 states, $\sim$2000 cm^{-1} as recently measured,[9] a 10 ps lifetime of the IS state appears overestimated.

In conclusion, the exact interaction of the $T_2(\pi,\pi^*)$ state with both the $T_1(n,\pi^*)$ triplet and the $S_1(n,\pi^*)$ singlet on the full relaxation mechanism of the latter is probably one of the key points to answer the controversy studied in this paper. In this sense, a recent advanced CASSCF calculation on carbonyl compounds has revealed the existence of a $S_1/T_1/T_2$ surface intersection that may play a crucial role in the relaxation dynamics upon photoexcitation,[35] but it is not clear whether this can possibly be related to a detectable intermediate species during the relaxation mechanism of the S_1 state of BP or not. New experimental and theoretical efforts are required to definitively answer this question and some of those raised in this paper.

Acknowledgment. The authors acknowledge Prof. A. de Juan from the Department of Analytical Chemistry of the Universitat de Barcelona for making available the modification of the MATLAB code for the implementation of hard-modeling constraint in MCR-ALS. The authors are grateful to B. N. Shivakiran Bhaktha for help with the revision of the English version. L.B. acknowledges a PhD scholarship from the Ministère délégué à l'Enseignement supérieur et à la Recherche, France. The authors thank the Groupement de Recherche GDR 2466 from CNRS and the Centre d'études et de Recherches Lasers et Applications (CERLA) for their help in the development of this work. CERLA is supported by the Ministère chargé

de la Recherche, Région Nord/Pas de Calais, and the Fonds Européen de Développement Economique des Régions.

References and Notes

(1) (a) Hochstrasser, R. M.; Lutz, H.; Scott, G. W. *Chem. Phys. Lett.* **1974**, *24*, 162. (b) Anderson, R. W.; Hochstrasser, R. M.; Scott, G. W. *Chem. Phys. Lett.* **1974**, *28*, 153. (c) Damschen, D. E.; Merritt, C. D.; Perry, D. L.; Scott, G. W.; Talley, L. D. *J. Chem. Phys.* **1978**, *82*, 2268.

(2) Greene, B. I.; Hochstrasser, R. M.; Weisman, R. B. *J. Chem. Phys.* **1979**, *70*, 1247.

(3) Hamanoue, K.; Nakajima, K.; Hidaka, T.; Nakayama, T.; Teranishi, H. *Laser Chem.* **1984**, *4*, 287.

(4) Miyasaka, H.; Morita, K.; Kamada, K.; Mataga, N. *Bull. Chem. Soc. Jpn.* **1990**, *63*, 3385.

(5) McGarry, P. F.; Doubleday, C. E., Jr.; Wu, C-H.; Staab, H. A.; Turro, N. J. *J. Photochem. Photobiol. A* **1994**, *77*, 109.

(6) Prater, K.; Freund, W. L.; Bowman, R. M. *Chem. Phys. Lett.* **1998**, *295*, 82.

(7) Shah, B. K.; Rodgers, M. A. J.; Neckers, D. C. *J. Phys. Chem. A* **2004**, *108*, 6087.

(8) Turro, N. J. *Modern Molecular Photochemistry*; The Benjamin/Cummings Publishing Company: 1978.

(9) Yabumoto, S.; Sato, S.; Hamaguchi, H. *Chem. Phys. Lett.* **2005**, *100*, 416.

(10) El-Sayed, M. A.; Leyerle, R. *J. Chem. Phys.* **1975**, *62*, 1579.

(11) Wäckerle, G.; Bär, M.; Zimmermann, H.; Dinse, K.-P.; Yamauchi, S.; Kashmar, R. J.; Pratt, D. W. *J. Chem. Phys.* **1982**, *76*, 2275.

(12) Tauler, R. *Chemom. Intell. Lab. Syst.* **1995**, *30*, 133.

(13) Navea, S.; de Juan, A.; Tauler, R. *Anal. Chem.* **2003**, *75*, 5592.

(14) Ruckebusch, C.; Duponchel, L.; Sombret, B.; Huvenne, J. P.; Saurina, J. *J. Chem. Inf. Comput. Sci.* **2003**, *43*, 1966.

(15) Blanchet, L.; Mezzetti, A.; Ruckebusch, C.; Huvenne, J. P.; de Juan, A. *Anal. Bioanal. Chem.* **2007**, *387*, 1863.

(16) Von Frese, J.; Kovalenko, S. A.; Ernsting, N. P. *J. Chemom.* **2007**, *21*, 2.

(17) Zhang, L.; Quan, D.; Wang, L.; Yang, G.; Weng, Y. *Sci. China G* **2004**, *47*, 208.

(18) (a)Van Stokkum, I. H. M.; Scherer, T.; Brouwer, A. M.; Verhoeven, J. W. *J. Phys. Chem.* **1994**, *98*, 852. (b) Vengris, M.; Van Stokkum, I. H. M.; He, X.; Bell, A. F.; Tongue, P. J.; Van Grondelle, R.; Larsen, D. S. *J. Phys. Chem. A* **2004**, *108*, 4587.

(19) Plaza, P.; Mahet, M.; Martin, M. M.; Checcucci, G.; Lenci, F. *J. Phys. Chem. B* **2004**, *108*, 6087.

(20) Malinowski, E. R. *Factor Analysis in Chemistry*, 2nd ed.;Wiley-Interscience: New York, 1992.

(21) De Juan, A.; Casassas, E.; Tauler, R. In *Encyclopedia of Analytical Chemistry*; Meyers, R. A., Ed.; John Wiley and Sons Ltd: Chichester, 2000; p 9800.

(22) De Juan, A.; Maeder, M.; Martinez, M.; Tauler, R. *Chemom. Intell. Lab. Syst.* **2002**, *54*, 123.

(23) Amigo, J. M.; de Juan, A.; Coello, J.; Maspoch, S. *Anal. Chim. Acta* **2006**, *567*, 245.

(24) Boscà, F.; Cosa, G.; Miranda, M. A.; Scaiano, J. C. *J. Photochem. Photobiol. Sci.* **2002**, *1*, 704.

(25) Golub, G. H.; Van Loan, C. F. *Matrix computations*, 2nd ed.; John Hopkins University Press: Baltimore, 1990; Chapter 8.

(26) Maeder, M. *Anal. Chem.* **1987**, *59*, 527.

(27) Ruckebusch, C.; Aloïse, S.; Blanchet, L.; Huvenne, J. P.; Buntinx, G. *Chem. Intell. Lab. Syst.*, to be published, DOI:10.1016/j.chemolab.2007.05.007.

(28) Maeder, M.; Neuhold, Y. M. *Practical Data Analysis in Chemistry*, Rutan, S., Walczak, B., Eds.; Elsevier: New York, 2007; Chapter 4.

(29) Jaumot, J.; Gemperline, P. J.; Stang, A. *J. Chemom.* **2005**, *19*, 97.

(30) Kovalenko, S. A.; Schanz, R.; Farztdinov, V. M.; Hennig, H.; Ernsting, N. P. *Chem. Phys. Lett.* **2000**, *323*, 312.

(31) Sun, Y. P.; Sears, D. F.; Saltiel, J. *J. Am. Chem. Soc.* **1989**, *111*, 706.

(32) Batley, M.; Kearns, D. R. *Chem. Phys. Lett.* **1968**, *2*, 423.

(33) Nakayama, T.; Sakurai, K.; Ushida, K.; Kawatsura, K.; Hamanoue, K. *Chem. Phys. Lett.* **1989**, *164*, 557.

(34) Singh, A. K.; Bhasikuttan, A. C.; Palit, D. K.; Mittal, J. P. *J. Phys. Chem. A* **2000**, *104*, 7002.

(35) He, H-Y.; Fang, W-H.; Philips, D. L. *J. Phys. Chem. A* **2004**, *108*, 5386.